THE INFLUENCE OF BITUMINOUS COAL AND OVERBURDEN THERMO-MECHANICAL PROPERTIES ON SUBSIDENCE ASSOCIATED WITH UNDERGROUND COAL CONVERSION

Harold D. Shoemaker[1]
Sunder H. Advani[2]
Frank D. Gmeindl[2]
Yang-Tsi Lin[2]

[1]Morgantown Energy Research Center
Morgantown, West Virginia 26505

[2]West Virginia University
Morgantown, West Virginia 26505

INTRODUCTION

The in situ conversion of coal into combustible gas provides an attractive avenue for optimum utilization of the United States' principal fossil fuel resource. The primary benefits of underground coal gasification (UCG) over conventional mining methods are health, safety, controlled environmental subsidence, and maximum recovery of energy from coal deposits which are difficult to mine or are unminable. The success of UCG methods from environmental, technical, and economic considerations depends on a host of physical, chemical, and geological parameters. These factors have been extensively discussed in monographs detailing Soviet technology (1,2) and the recent British National Coal Board Status review of studies in the United Kingdom, Russia and United States (3). The major U.S. Department of Energy (DOE) sponsored projects in the United States are the Linked Vertical Well (LVW) programs at Hanna, Wyoming (4), and at Pricetown, West Virginia (5), in the medium thick western and thin eastern coal seams, respectively; and the Packed Bed Process (PBP) experiments near Gillette, Wyoming (6), also in the thick western coal seams.

The surface and subsurface environmental impact of in situ coal gasification may be predicted by utilizing the thermo-mechanical-structural properties of the in situ materials. The most serious structural mechanics related problems of UCG are those dealing with surface subsidence, roof stability, and coal permeability thermo-mechanical changes. The ensuing subsurface environmental consequences include possible gas leakage, water contamination, water influx into the combustion zone, and heat loss to the overburden. Control of the UCG process rate advancement, its stability, and surface and subsurface subsidence response is believed to be primarily due to the thermally induced strain and in situ stresses. In addition, coalbed permeabilities in the swelling bituminous coals are also influenced (7). Hence, the basic structural and constitutive properties of the in situ materials must be known in order to predict the effects of a gasification scheme with regard to roof collapse, coal fracturing, porosity, permeability, and surface subsidence.

This study represents an effort to provide somewhat more realistic and comprehensive experimental data of in situ gasification materials for utilization in subsidence comparisons from various empirical and phenomenological theories for the stratigraphy conforming to the Morgantown Energy Research Center (MERC) UCG experiments. An elastic finite element theory with specified failure criteria is used to identify the surface displacements, surface strains, and roof and surface failure zones.

PREVIOUS INVESTIGATIONS

Most of the research performed to determine the strength of coal has been from uniaxial compression tests on cubical, rectangular, or irregular shaped specimens (8,9,10). Coal has a greater ultimate compressive strength when loaded normal to the bedding planes than when loaded normal to either the face or butt cleats (8,9).

The ultimate strength increases when the stresses become representative of in situ tectonic stresses as shown from triaxial loading experiments (9,11,12,13). The ultimate compressive strength of coal whether loaded normal to the bedding planes or the cleat planes is test specimen size dependent (14,15,16), and increases exponentially with decreasing specimen size.

Similarly, there are many widely used shapes and sizes in determining the mechanical properties of rock; such as, cylinders, prisms and plates (17-25). The various studies on rock do not support the size dependence as shown in coal (22,23,26-31); that is, an increase in specimen size may or may not affect the ultimate strength of rock. However, under triaxial loading conditions the size effects are only present for low confining pressures (32).

There is evidence that coal and rock are viscoelastic materials and that coal behaves like a viscous fluid at elevated temperatures. Brewer (33) states that when bituminous coal is heated under appropriate conditions, it may exhibit plastic, viscous, or elastic flow, and often combinations of all three. Macrae and Mitchell (34) reported that the ultimate failure stress and deformation were notably time dependent. At room temperature, failure occurred after a high stress had been maintained on the specimen for an extended period of time. Sanada and Honda (35) have demonstrated that the time-temperature superposition principle can be applied to coal. Singh (36) demonstrated the three stages (primary, secondary, and tertiary) of the idealized creep curve in rock.

The utilization of thermo-mechanical properties of the involved materials in the application of subsidence and strata control theories, to underground mining, in the United States is relatively recent. The pioneering pre-World War II German experience and European efforts on pre-calculation of coal mine subsidence (37-41) have served as blueprint characterizations for sophisticated modeling. The techniques for predicting mine subsidence are based either on mathematical representations for the continuous trough profile or the influence function expressing the extraction of infinitisimal elements. A comprehensive survey of these methods and vertical subsidence S(x) computations for several profile or influence functions are given by Brauner (42). The empirical relations

$$V(x) = C_1 \ (dS/dx) \qquad 1)$$

and

$$E(x) = C_1 d^2S/dx^2 \qquad 2)$$

are employed for evaluation of the horizontal displacement V(x) and the horizontal surface strain E(x). Brauner (42) also presents considerations for time dependent and inclined strata subsidence behavior. The Subsidence Engineers' Handbook (43) furnishes extensive field results and design curves for predicting displacements, tilts, and strains. For critical or super critical widths, the maximum vertical subsidence S_{max} is generally from 0.50 to 0.90 of the seam thickness while the maximum horizontal displacement V_{max} is about one-third of S_{max}. The corresponding maximum tilt, compressive strain, and tensile strain values are approximately 2.5 S_{max}/depth, 0.5 S_{max}/depth, and 0.67 S_{max}/depth, respectively.

The mine subsidence representations discussed in the literature sited above are primarily semi-empirical and do not address local geo-mechanical variables. Various phenomenological model representations have been attempted to include geometric and material property effects. These investigations encompass two- and three-dimensional linear isotropic and anisotropic elasticity theory models (44-48), viscoelastic responses (49), experimental models (50), and elastic as well as elasto-plastic finite element model subsidence evaluations (51-53) utilizing experimental field data. Several roof stress response studies relating to underground opening design and mining operations have been conducted utilizing the finite element stress evaluations (54-56). Similar studies on the influence of stresses on roof rock fractures, block boundary weakening, and cavability have been conducted (57). Other investigators (1)

and reports (2) have also presented qualitative discussions relative to surface subsidence, roof collapse and the ensuing technical and environmental problems.

EXPERIMENTAL STUDIES

In examining structural property effects on subsidence, roof collapse, and various modes of failure, specific types of data are required. The basic properties required are directional (for coal) and temperature-dependent stress-strain relations and failure stresses in compression and shear.

The Pittsburgh bituminous coal and its adjacent overburden were evaluated in the experiments. All experiments were conducted in uniaxial compression and simple shear, in determining both the elastic and viscoelastic properties of the materials. Because of the size dependency of coal with regard to its ultimate strength, four different specimen sizes, ½" x ½" x 1", 1" x 1" x 2", 2" x 2" x 4", and 4" x 4" x 8" (1.27 x 1.27 x 2.54 cm, 2.54 x 2.54 x 5.08 cm, 5.08 x 5.08 x 10.16cm, and 10.16 x 10.16 x 20.32 cm), were used in the uniaxial compression tests and one in simple shear, ½" x 2" x 2" (1.27 x 5.08 x 5.08 cm) (figure 1). One specimen size was used in the overburden experiments in uniaxial compression, ½" x ½" x 1" (1.27 x 1.27 x 2.54 cm). The thermo-mechanical properties test apparatus and experimentation details are described elsewhere (58).

Elastic Experiments -- Temperature has a dramatic effect upon the ultimate strength and ultimate strain of coal and the overburden (figures 2-4). Regardless of specimen size, the ultimate strength of the coal is greatest at 200°F (93°C) (figure 2). The dark gray shale, which contains carbon, responds similarly to coal in that the largest ultimate strength is shifted to the right to approximately 350°F (177°C), while the light gray shale displays progressively increased strength as the temperature increases over the temperature range obtained (75°-700°F (24°-371°C)). The ultimate strain is relatively constant for the coal and dark gray shale until the temperature of the specimens exceed 500°F (260°C) and 575°F (302°C), respectively, where large finite strains occur; while for the light gray shale the ultimate strain remains relatively constant over the temperature range investigated (75°-700°F (24°-371°C)) (figures 2 and 3). Notice, figure 4, the characteristic S-shape of the stress-strain curves and the elasto-plastic response of the coal to uniaxial compressive loading.

Theory does not support the phenomen observed in the coal and dark gray shale that their strengths increase with temperature before a final decrease to very small values (figures 2-4). However, these characteristics have been observed in coal (34) and dark gray shale (59). Macrae and Mitchell (34) postulated that the increased strength at approximately 212°-248°F (100°-120°C) was due to the weaker secondary forces of the van der Waals-type between structural units being affected and that heating affects the mode of fracture from tension at ordinary temperatures to shear at temperatures above 212°F (100°C). These results were generally validated in the experiments.

The ultimate shearing strengths from the shear tests were, in general, independent of the orientation of loading (varied less than 200 psi (0.138×10^7 N/m^2) over the temperature range) (figure 5). The results for loadings normal to the face and butt cleats in uniaxial compression are also similar, but different from loadings normal to the bedding planes (figure 6). This similarity indicates that at least along these two directions the Pittsburgh coal behaves as a transversely isotropic material as also observed (9,35,60) for other coals.

Viscoelastic Experiments -- The viscoelastic properties of the coal and overburden also represent a large variety of linear and nonlinear rheological properties. The effect of orientation of the constant applied load on the creep compliance in coal is demonstrated in figure 7 at 500°F (260°C). Notice, the difference between the

curves, compressive loading normal to the bedding planes demonstrates failure in tertiary creep after approximately six minutes, while for loadings normal to the face and butt cleats failure did not occur until much later (35 minutes). This directional effect is apparently due to increased resistance to deformation in the face and butt cleat directions caused by the interlayering of the organic and inorganic materials when the loading is parallel to the bedding planes. The Pittsburgh coal can also be represented by the time-temperature superposition principle (figure 8).

ROOF RESPONSE EVALUATIONS AND SUBSIDENCE COMPUTATIONS

The presented experimental data is employed for the evaluation of UCG fractured roof zones, roof convergence, and surface subsidence. Figure 9a reveals the selected two-dimensional model corresponding to the planned Morgantown Energy Research Center line-drive experiments at Pricetown, West Virginia. Figure 9b illustrates the propagating cavity configuration at a specified time instant with the adjacent coke, softened layers, and overburden. The corresponding "steady state" constant temperature profiles, computed by the Alternating Direction Implicit Method (61) are shown in figure 9c.

The stress model simulations entail use of the NASTRAN finite element code for an initially selected cavity configuration at time t_1. The effects of temperature loading, in situ stresses, and internal pressure are superposed and temperature dependent mechanical properties are assumed for the Pittsburgh coal and overburden shale elements. On the basis of the computer principle stresses, failure criteria in terms of the tensile and compressive yield strengths are applied as follows.

Compression Failure -- This failure occurs when

$$C_o = \sigma_3 - \sigma_1 \left[\frac{(1 + \mu_f^2)^{\frac{1}{2}} + \mu_f}{(1 + \mu_f^2)^{\frac{1}{2}} - \mu_f} \right] \qquad 3)$$

where σ_1 and σ_3 are the major and minor principal stresses, respectively, C_o is the uniaxial compressive strength, and μ_f is the internal coefficient of friction.

Tension Failure -- For the case $3\sigma_1 + \sigma_3 > 0$, the limiting failure criterion is

$$\sigma_1 = T_o \qquad 4)$$

where T_o is the uniaxial strength in tension.

Shear Failure -- For the case $3\sigma_1 + \sigma_3 < 0$, failure is governed by

$$-(\sigma_1 - \sigma_3)^2(\sigma_1 + \sigma_3)^{-1} = 8T_o \qquad 5)$$

At the initial specified time instant, the elastic model is simulated and the failure zones are identified. The elastic properties of these failure regions are then reduced by a factor of 100 since the normal horizontal stresses are relieved. The resulting stress distributions, roof convergence, and surface subsidence values are determined. The procedure is continued until maximum roof convergence is obtained. For each subsequent time instant, this method is repeated and the new corresponding failure zones are obtained along with the roof convergence profile and surface subsidence.

The selected mechanical and thermal properties for the model simulation are presented in table 1 and figure 10. The roof and coal failure zones for different time instants computed from the NASTRAN model simulation and assigned failure criteria are illustrated in figure 11. The corresponding non-dimensionalized elastic and "fractured" roof convergence profiles are revealed in figure 12 with the vertical surface subsidence profiles shown in figure 13.

TABLE I. Selected Mechanical and Thermal Properties for the Master Model.

Property	Symbol	Units	Coal	Softened Coal Layer	Coke	Sandstone	Light Gray Shale	Dark Gray Shale
Young's Modulus	E	psi (N/m^2)	186×10^3 (128×10^7)	500 (0.345×10^7)	130×10^3 (89.6×10^7)	2.0×10^6 (1.38×10^{10})	800×10^3 (552×10^7)	See Figure 10
Poisson's Ratio	ν	---	0.44	0.47	0.25	0.12	0.15	0.45
Thermal Expansion Coefficient	α	$/^oF$ ($/^oC$)	2.78×10^{-6} (5.00×10^{-6})	5.40×10^{-6} (9.72×10^{-6})	4.50×10^{-6} (8.10×10^{-6})	4.50×10^{-6} (8.10×10^{-6})	4.50×10^{-6} (8.10×10^{-6})	4.50×10^{-6} (8.10×10^{-6})
Thermal Conductivity	K	Btu/^{o}F-in-sec (Kgcal/^{o}C-m-sec)	2.79×10^{-6} (4.98×10^{-5})	5.15×10^{-6} (9.20×10^{-5})	7.50×10^{-6} (13.4×10^{-5})	2.50×10^{-6} (4.47×10^{-5})	2.50×10^{-6} (4.47×10^{-5})	2.50×10^{-6} (4.47×10^{-5})
Mass Density	ρ	lbm/in^3 (Kg/m^3)	0.046 (1,273)	0.028 (775)	0.037 (1,024)	0.070 (1,938)	0.078 (2,159)	0.078 (2,159)
Compressive Strength	Small Specimen C_o	psi (N/m^2)	4,000 (2.76×10^7)	----	----	14,000 (9.65×10^7)	14,000 (9.65×10^7)	14,000 (9.65×10^7)
Compressive Strength	Scaled C_o	psi (N/m^2)	2,800 (1.93×10^7)	----	----	2,800 (1.93×10^7)	2,800 (1.93×10^7)	2,800 (1.93×10^7)
Tensile Strength	Small Specimen T_o	psi (N/m^2)	430 (0.3×10^7)	----	----	430 (0.3×10^7)	430 (0.3×10^7)	430 (0.3×10^7)
Tensile Strength	Scaled T_o	psi (N/m^2)	86 (0.06×10^7)	----	----	86 (0.06×10^7)	86 (0.06×10^7)	86 (0.06×10^7)

DISCUSSION AND CONCLUSIONS

The tests conducted on the Pittsburgh coal and adjacent overburden were conventional ones used for determining the properties identified for elastic or viscoelastic isotropic, homogeneous materials. The data from these tests represent a large variety of linear and nonlinear rheological properties including plasticity and creep, depending upon temperature. In reality, the Pittsburgh coal and dark gray shale behave as plastic, elasto-plastic viscoelastic materials under different conditions and none of the existing elasto-plastic or other known plastic theories are suitable for totally describing the stress-strain-time characteristics. Similar phenomena have been described by others (33-35).

These experimentally obtained Pittsburgh coal and overburden thermo-mechanical properties furnish basic data for the detailed structural simulation of the roof and surface subsidence responses during in situ gasification processes. A related study (62), utilizing an elasto-plastic finite element model with temperature independent overburden properties, has demonstrated that the maximum surface subsidence is 0.52 X seam thickness (for the two-dimensional plane strain model stratigraphy simulated here with a 500 foot (152 m) extraction width). The corresponding yielded zone extends to a distance of approximately 350 feet (107 m) immediately above the roof. This value apparently represents an upper bound since conservative overburden compressive and tensile structural strengths are used (C_o = 2800 psi (1.93×10^7 N/m^2) and T_o = 86 psi (0.06×10^7 N/m^2)). For the simulations presented here, the surface subsidence corresponding to an extracted width of 100 feet (30.5 m) is 0.14 X seam thickness (figure 13) with a vertical overburden fractured shear and tensile zone of approximately 36 feet (11 m) (figure 11). Related studies (61,62) have been conducted on crack propagation in the overburden roof rock. This thermal cracking of the roof block provides an avenue for water influx into the combustion zone to enhance the heating value of the produced gas. However, gas leakage to the surface, via the thermal cracks and the tensile and shear induced fissures in the roof, does not appear probable for this case. The magnitudes and slopes of the roof convergence profiles in figure 12 are important indicators of the intermittent roof fracturing process. The propagation of the combustion front is enhanced by the severe compressive stress concentrations induced at the cavity edge (figure 11, the Longwall Generator

underground gasification concept is here represented). Similar stress analysis considerations also apply to the Linked Vertical Well gasification concept with a tear drop shaped cavity. The corresponding sweep areas are limited for thin seam coal since the radial combustion velocities are limited and the resulting roof stress concentrations are considerably less severe than for the Longwall Generator case.

These thermo-mechanical data also become useful in understanding the basic mechanisms involved in mass and energy transport and mechanical-structural effects in gasification processes. For example, decreased permeability shortly after initiation of a burn in modeling coal gasification processes in the laboratory with the Pittsburgh coal and overburden is readily understood to be due to the swelling and effervescent nature (bubbling of tars into the fissures) of the Pittsburgh coal at elevated temperatures. The tars, along with the swelling of the Pittsburgh bituminous coal, tend to restrict the outward movement (reduce permeability) of the combustion front around a borehole or cavity as well as inhibit a forward burn along a borehole. However, the swelling, effervescent and coalescent nature of the Pittsburgh coal becomes an asset in control of channeling or short-circuiting in line-drive gasification processes (7) in that the fluidic coal will be forced into these channels by the pressure of the fractured roof (overburden) and the swelling of the coal.

Although water influx effects into the combustion zone are not explicitly considered in the subsidence analysis, the additional subsidence due to extraction of the neighboring fluids can be included by assigning the ratio of the depleted fluid volume during gasification to the caved block volume (62). The subsidence curve can then be accordingly modified.

REFERENCES

1. Skafa, P. V., "Underground Gasification of Coal," Gosudarstvenno Hauchno-Tekhnicheskoe Izdatel'stvo Literatury Po Gornomu Delu, Moscow (1960); also UCRL-TRANS-10880, September 1975, 324 pp.
2. Anon, "A Current Appraisal of Underground Coal Gasification," PB 209 274, Arthur D. Little, Inc., Cambridge, Mass., 1972.
3. Thompson, P. N., Mann, J. R., and F. Williams, "Underground Gasification of Coal," National Coal Board, UK, 1976.
4. Schrider, L. A. and D. D. Fisher, "In Situ Coal Gasification - A Unique Means for Energy Recovery," ASME Paper No. 75-PVP-44, 1975.
5. Strickland, L. D., "A Status Report on MERC's Program for In Situ Gasification of Bituminous Coals," presented at 3rd Annual Underground Coal Gasification Symposium, sponsored by Lawrence Livermore Laboratory at Fallen Leaf Lake, CA, June 6-10, 1977, 13 pp.
6. Stephens, D. R., "LLL In Situ Coal Gasification Program - Annual Report 1975," UCRL-50032-75, Lawrence Livermore Laboratory, Livermore, CA, 1975.
7. Advani, S. H., L. Z. Shuck, and K. Y. Lee, "Stress Response Investigations Related to In Situ Gasification of Coal," in press, ASME transactions, paper presented at the Energy Technology Conference and Exhibition, Houston, TX, September 18-22, 1977, Paper No. 77-Pet-25, 5 pp.
8. Evans, I. and C. D. Pomeroy, "The Compressive Strength of Rectangular Blocks of Coal," National Coal Board (England), Report 2077, October 1957, 15 pp.
9. Evans, I. and C. D. Pomeroy, "The Strength, Fracture, and Workability of Coal," Pergamon Press, New York, 1966, 277 pp.
10. Rad, P. F., "Mechanical Properties and Cutting Characteristics of Coal," BuMines Information Circular 8584, 1973, 46 pp.
11. Hobbs, D. W., "Strength and Stress-Strain Characteristics of Coal in Triaxial Compression," J. Geol., v. 72, March 1964, pp. 214-231.
12. Pomeroy, C. D. and D. W. Hobbs, "Fracture of Coal Specimens Subjected to Complex Stresses," Steel and Coal, v. 185, December 1962, pp. 1124-1133.

13. Ko, Hon-Yim and K. H. Gerstle, "Elastic Properties of Two Coals," Internat. Journal of Rock Mechanics, Mineral Science, and Geomechanics, v. 13, 1976, pp. 81-90.
14. Bieniawski, Z. T., "Effect of Specimen Size on Compressive Strength of Coal," Internat. Journal of Rock Mechanics and Mineral Science, v. 5, July 1968, pp. 325-335.
15. Evans, I., C. D. Pomeroy, and R. Berenbaum, "Compressive Strength of Coal," Coal, Eng., v. 38, 1961, pp. 75-87.
16. Gaddy, F. L., "Study of Ultimate Strength of Coal as Related to Absolute Size of Cubinal Specimens Tested," Va. Polytechnical Inst., Eng. Expr. Sta., Ser. 112, August 1956, 27 pp.
17. Narayanan R., "Some Factors which affect Concrete Strength," Cement and Concrete 2, 71-82, 1961.
18. Symons, I. F., "The Effect of Size and Shape of Specimen upon the Unconfined Compressive Strength of Cement-Stabilised Materials," Magazine of Concrete Research 22, 45-50, 1970.
19. Kadlecek, V. and Z. Spetla, "Effect of Size and Shape of Test Specimens on the Direct Tensile Strength of Concrete," RILEM Bulletin, No. 36, 175-184, 1967.
20. Bieniawski, Z. T., "The Compressive Strength of Hard Rock," CSIR Report MEG 272, Pretoria, 1968.
21. Gonnerman, H. F., "Effect of Size and Shape of Test Specimens on Compressive Strength of Concrete," Proc. ASTM 25, 237-250, 1925.
22. Hoskins, J. R. and F. G. Horino, "Influence of Spherical Head Size and Specimen Diameters on the Uniaxial Compressive Strength of Rocks," BuMines RI 7234, 1969.
23. Dhir, R. K., C. M. Sangha and J. G. L. Munday, "Influence of Specimen Size on Unconfined Rock Strength," Colliery Guardian 220, 75-80, 1972.
24. Robertson, E. C., "Experimental Study of the Strength of Rocks," Bull. Geol. Soc. Am. 66, 1275-1314, 1955.
25. Fumagalli, E., discussion on a paper by Iyenger et al—"Strength of Concrete under Biaxial Compression," Journal of the Am. Concrete Inst., Proc. 62, 1187-1189, 1965.
26. Obert L., S. L. Windes, and W. I. Duvall, "Standardized Tests for Determining the Physical Properties of Mine Rock," US BuMines RI 3891, 1946.
27. Skinner, W. J., "Experiments on the Compressive Strength of Anhydrite," The Engineer 207, 255-259 and 288-292, 1959.
28. Mogi, K., "The Influence of the Dimensions of Specimens on the Fracture Strength of Rocks," Bull. Earthquake Res. Inst., Tokyo Univ. 40, 1975-185, 1962.
29. Hodgson, K. and N. G. W. Cook, "The Effects of Size and Stress Gradient on the Strength of Rock," Proc. Second Congress Int. Soc. Rock Mech. Belgrade 2, 31-34, 1970.
30. Stamatiu, M. and C. C. Teodorescu, "Quelques Properties Physiques et Mecaniques du sel Gemme Roumain," Proc. Seventh Congr. Int. Min. Met. Geol. Appl., Paris 1, 317-320, 1935.
31. Ruhfus, B., "Investigation of the Influence of the Dimensions and Layering of Rock Specimens upon the Compressive Strength," M.S. Thesis, Colorado School of Mines, 1961.
32. Habib, P. and G. Vouille, "Sur la Disparition de l'Effect d'Echelle aux Hautes Pressions," Cr. hebd. Seanc. Acad. Sci., Paris, 1966.
33. Brewer, R. E., "Plastic and Swelling Properties of Bituminous Coking Coals," BuMines Bulletin 445, 1942, 260 pp.
34. Macrae, J. C. and A. R. Mitchell, "The Response of Bright Bituminous Coal to Undirectional Compression," Fuel, v. 36, October 1957, pp. 423-441.
35. Sanda, Y. and H. Honda, "Creep in Coal Over the Temperature Range 200 to 370°C," Fuel, v. 42, 1963, pp. 479-486.
36. Singh, D. P., "A Study of Creep of Rocks," Int. J. Rock Mech., Min. Sci., and Geomech. Abstr., v. 12, pp. 271-276, 1975.
37. Briggs, H., "Mining Subsidence," E. Arnold and Co., London, 215 pp., 1929.
38. Bals, R., "A Contribution to the Problem of Precalculating Mining Subsidences," Mitteilungen aus dem Markscheidewesen, v. 42/43, pp. 98-111, 1931/1932.

39. Knothe, S., "Observations of Surface Movements under Influence of Mining and Their Theoretical Interpretation," Proceedings of the European Congr. on Ground Movement, Univ. of Leeds, pp. 49-57, 1957.
40. Drent, S., "Some Considerations on the Connection Between Time-Curves and the Thickness of the Non-Carboniferous Overburden in the South Limburg Coalfield," Proc. of European Congr. on Ground Movement, Univ. of Leeds, pp. 49-57, 1957.
41. Zenc, M., "Comparison of Bals' and Knothe's Methods of Calculating Surface Movements Due to Underground Mining," Internat. J. of Rock Mech. & Min. Sci., v. 6, pp. 159-190, 1969.
42. Brauner, G., "Subsidence Due to Underground Mining," Part I: "Theory and Practices in Predicting Surface Deformation," Part II: "Ground Movements and Mining Damage," BuMines Info Circ. 8571, 8572, 1973.
43. "Subsidence Engineers' Handbook," Nat. Coal Board Mining Department, 1975.
44. Berry, D. A. and T. W. Sales, "An Elastic Treatment of Ground Movement due to Mining-II, Transversely Isotropic Ground," J. of Mech. & Phys. of Solids, v. 9, pp. 52-62, 1961.
45. Berry, D. A. and T. W. Sales, "An Elastic Treatment of Ground Movement Due to Mining-III, Three-Dimensional Problem, Transversely Isotropic Ground," J. of Mech. & Phs. of Solids, v. 10, pp. 73-83, 1962.
46. Berry, D. A., "The Ground Considered as a Transversely Isotropic Material," Internat. J. of Rock Mech. & Min. Sci., v. 1, pp. 159-167, 1964.
47. Salamon, M. D. G., "Elastic Analysis of Displacements and Stresses Induced by the Mining of Seam or Reef Deposits," J. of South African Inst. of Min. and Met., v. 64, pp. 128-129, pp. 197-218, pp. 468-500, 1963/1964.
48. Crouch, S. L. and C. Fairhurst, "Analysis of Rock Mass Deformations due to Excavations," Rock Mech. Symp., AMD-Vol. 3, ASME Pub., pp. 25-40, 1973.
49. Marshall, G. J., "A Visco-elastic Treatment of the Deformation of the Ground Caused by Mining Operations," J. of Mech. & Phy. of Solids, v. 17, pp. 151-162, 1969.
50. Pariseau, W. G. and H. D. Dahl, "Mine Subsidence and Model Analysis," Society of Mining Engineers, AIME, v. 241, pp. 488-494, 1968.
51. Brown, R. E., "A Multi-Layered Finite Element Model for Predicting Subsidence," PhD dissertation, Carnegie-Mellon Univ., Pittsburgh, PA, 1968.
52. Dahl, H. D., "A Finite Element Model for Anisotropic Yielding in Gravity Loaded Rock," PhD dissertation, the Penn. St. Univ., University Park, PA, 1969.
53. Mojumdar, B. K., "Mathematical Model of Ground Movement due to Underground Mining," PhD dissertation, the Penn. St. Univ., University Park, PA, 1974.
54. Kidybinski, A. and C. Babcock, "Stress Distribution and Rock Fracture Zones in the Roof of Longwall Face in a Coal Mine," Rock Mech., v. 5, pp. 1-19, 1973.
55. Kulhawy, F., "Finite Element Modeling Criteria for Underground Openings in Rock," Internat. J. of Rock Mech. & Min. Sci., v. 11, pp. 465-472, 1974.
56. Kulhawy, F., "Stress and Displacements Around Openings in Homogeneous Rock," Internat. J. of Rock Mech. & Min. Sci., v. 12, pp. 43-57, 1975.
57. Mahtab, M. and J. Dixon, "Influence of Rock Fractures and Block Boundary Weakening on Cavability," Soc. of Min. Engrs., AIME, v. 260, pp. 6-12, 1976.
58. Shoemaker, H. D., L. Z. Shuck, R. R. Haynes, and S. H. Advani," Directional Viscoelastic Properties of the Pittsburgh Coal at Elevated Temperatures in Compression and Shear," MERC/RI-76/5 (USERDA Rpt of Invest.), August 1976, 198 pp.
59. Baidyuk, B. V., "Mechanical Properties of Rocks at High Temperatures and Pressures," Gostoptekhizdat, Moscow, 1963 (translated by J. P. Fitzsimmons, Consultants Bureau, NY, 1967, 75 pp.).
60. Morgans, W. T. A. and N. B. Terry, "Measurement of Static and Dynamic Elastic Moduli of Coal," Fuel, v. 37, April 1958, pp. 201-219.
61. Advani, S. H., Y. T. Lin, V. Shah, and H. F. Wang, "Structural Mechanics and Model Simulations Associated with Underground Coal Gasification," proc. Am. Nuc. Soc. and ERDA Topical Mtg on Energy and Mineral Resource Recovery, 1977, in press.

62. Advani, S. H. and Y. T. Lin, "Subsidence and Roof Response Studies Related to Underground Coal Gasification," proc. 3rd Annual Underground Coal Conversion Symp., Fallen Leaf Lake, CA, June 1977, In press.

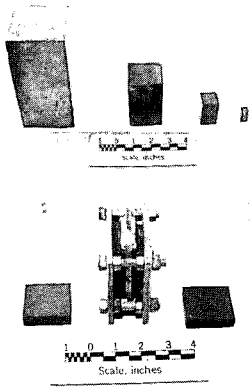

Figure 1. Pittsburgh Coal Specimens as Used in Uniaxial Compression and Shear Experiments.

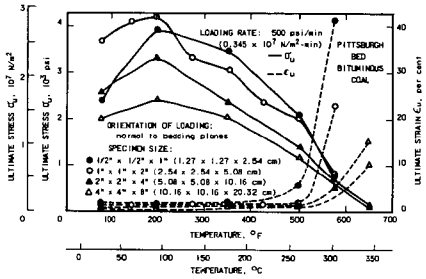

Figure 2. The Ultimate Stress and Strain-Temperature Curves Showing the Effect of Specimen Size of the Pittsburgh Coal When Loaded in Uniaxial Compression Normal to the Bedding Planes.

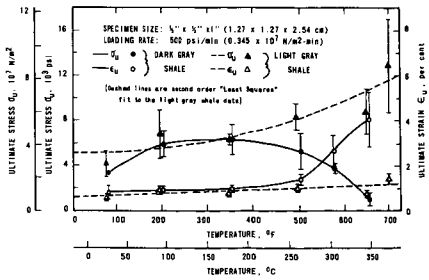

Figure 3. Ultimate Stress and Strain Curves as Functions of Temperature for Pittsburgh Seam Overburden When Loaded in Uniaxial Compression. The Bars on the Data Are ± One Standard Deviation.

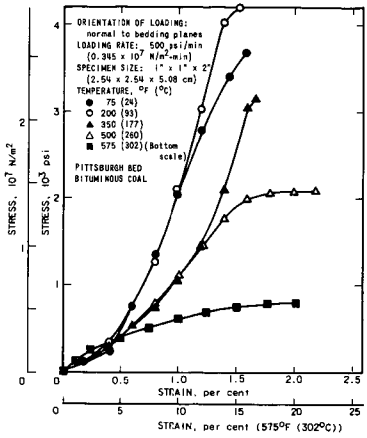

Figure 4. Stress-Strain Curves Loaded in Uniaxial Compression (Average Values) Showing the Effect of Temperature on the Pittsburgh Coal.

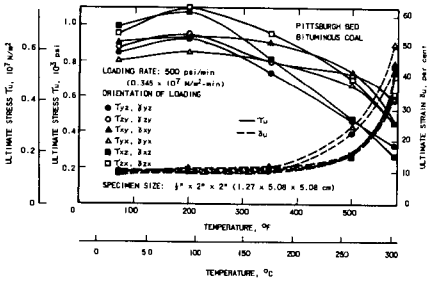

Figure 5. The Ultimate Stress and Strain-Temperature Curves Showing the Effect of Orientation of Loading in Shear on the Pittsburgh Coal.

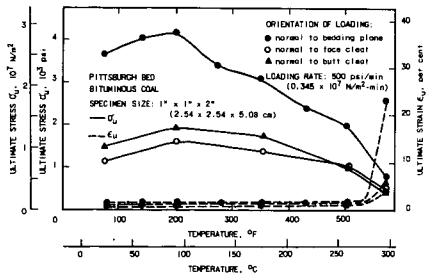

Figure 6. The Ultimate Stress and Strain-Temperature Curves Showing the Effect of Orientation of Loading on the Pittsburgh Coal When Loaded in Uniaxial Compression.

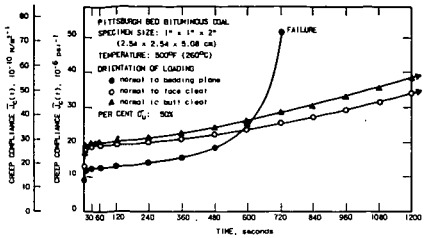

Figure 7. Creep Compliance-Time Curves Showing the Effect of the Orientation of Loading in Uniaxial Compression on the Pittsburgh Coal.

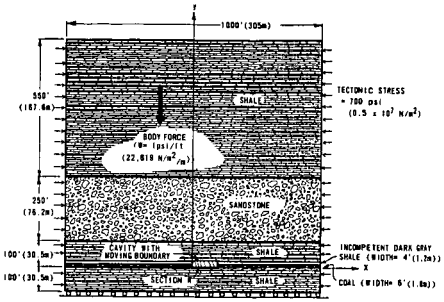

Figure 9a. The Master Model.

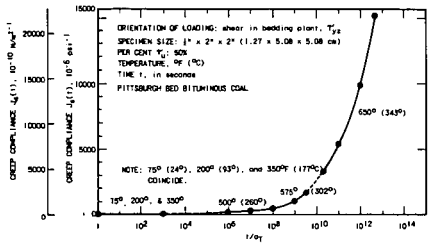

Figure 8. Time-Temperature Superposition Showing The Time Shift for the Pittsburgh Coal When Loaded in Shear.

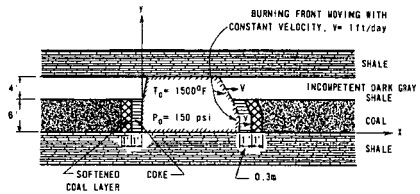

Figure 9b. Cavity with Moving Boundary (Section A) of the Master Model.

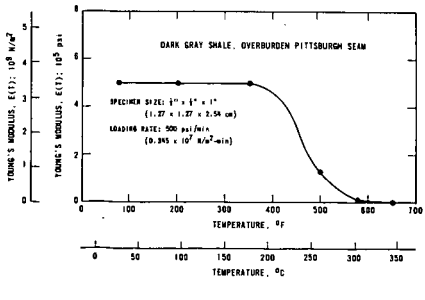

Figure 10. Young's Modulus for Dark Gray Shale as a Function of Temperature.

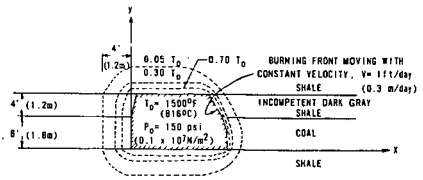

Figure 9c. Computed Steady State Temperature Distribution for the Master Model.

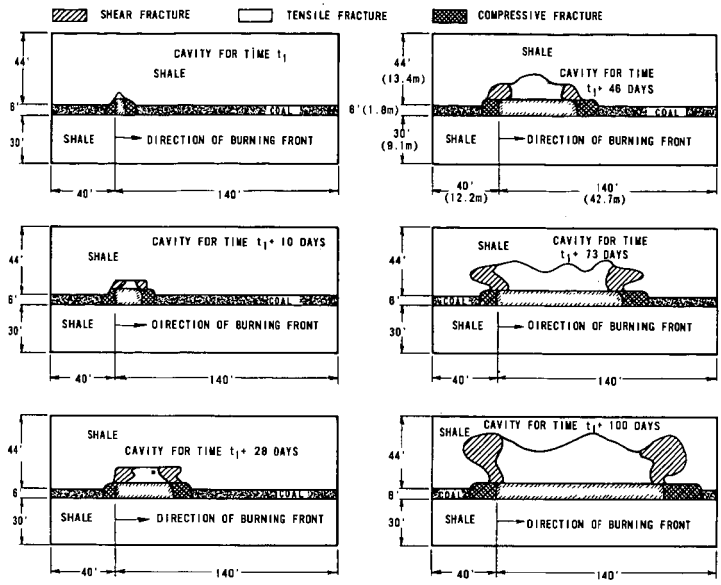

Figure 11. Failure Zones Adjacent to Cavity for Different Time Instants.

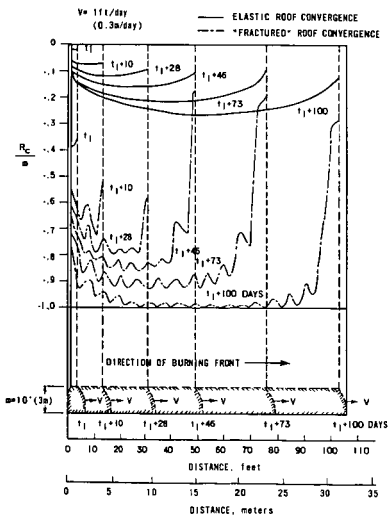

Figure 12. Roof Convergence Profiles for Different Burn Configurations.

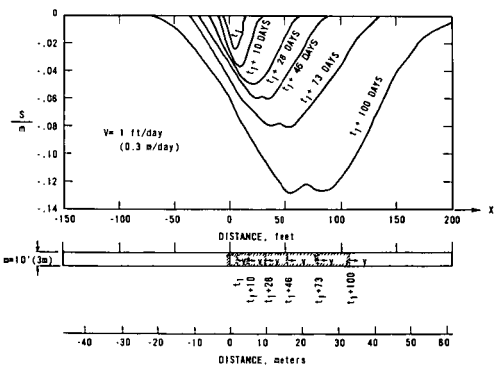

Figure 13. Surface Subsidence Profiles for Different Burn Configurations.